Latent Heat Recovery from Oxygen-Combustion Boiler

Masahiro OSAKABE*, Sachiyo HORIKI, Tugue ITOH
Tokyo University of Mercantile Marine, Koutou-ku, Tokyo 135-8533, Japan
Kunihiko MOURI
Electric Power Development Co., Ltd., Chuo-ku, Tokyo 104-8165, Japan

*corresponding author; Phone & FAX +81-3-5245-7408, E-Mail osakabe@ipc.tosho-u.ac.jp

The thermal hydraulic behavior was experimentally studied in a heat exchanger for the latent heat recovery from a flue gas exhausted from the oxygen-combustion boiler. The heat exchanger consisted of 2 staggered banks of 13 rows and 36 stages of spirally finned tubes. The parametric study varying the flue gas and feed water flow rate was conducted. The temperature distributions of cooling water and flue gas, the pressure loss and the amount of condensate were measured. Based on the previous basic studies, a thermal hydraulic prediction method was also proposed. For the condensation of steam on heat transfer tubes, the modified Sherwood number taking account of the mass absorption effect on the wall was proposed. The experimental results agreed well with the prediction proposed in this study. The total heat of 900kW including the latent heat of 730kW was successfully recovered in the present economizer specially designed for the oxygen-combustion boiler

Keyword: *Latent Heat Recovery, Oxygen-Combustion, Boiler, Thermal-Hydraulic Prediction*

Introduction

The most part of energy losses in a boiler is due to the heat released by the exhaust flue gas to atmosphere. The released heat consists of sensible and latent one. Recently, for a biological and environmental safety, a clean fuel such as a natural gas is widely used in the boiler. As the clean fuel includes a lot of hydrogen instead of carbon, the exhaust flue gas includes a lot of steam accompanying with the latent heat. As a next generation boiler, the oxygen combustion boiler was planned and developed in Japan. To reduce the total amount of exhaust flue gas and the toxic products generated with the combustion, it is preferable to use oxygen instead of air. Using the oxygen also can burn low-caloric gas. The oxygen-combustion flue gas has the larger amount of steam concentration than that in the air-combustion flue gas including nitrogen. So the latent heat recovery from the flue gas is very important to improve the boiler efficiency.

Shown in Fig.1 is the relation between the boiler efficiency and the exhaust gas temperature in the oxygen and air combustion system. The efficiency is larger than 100% at the lower exhaust temperature as the boiler efficiency is defined with a lower heating value of A-heavy fuel oil. The efficiency in the oxygen combustion is much higher than that in the air combustion due to the lack of heat loss carried out with the nitrogen. The dew point of the oxygen-combustion flue gas including the larger amount of steam instead of nitrogen is higher than that in the air-combustion flue gas. The steep increase of efficiency can be observed at the lower temperature region below the dew points. In this lower temperature region, the latent heat in the flue gas is recovered and the efficiency is increased. So the latent heat recovery from the flue gas is very important to improve the boiler efficiency in the oxygen combustion system.

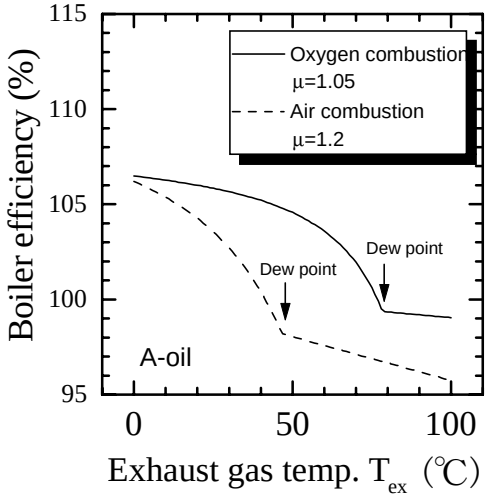

Fig. 1 Boiler efficiency in oxygen and air combustion

In the previous basic studies[1-4], condensation heat transfer on horizontal stainless steel tubes has been investigated experimentally by using an actual flue gas from a natural gas boiler. The experiments were conducted using single and 2 stages of tubes at different air ratios and steam mass concentrations of the flue gas in a wide range of tube wall temperature. The condensation heat transfer was well predicted with the simple analogy correlation in the high wall temperature region. In the low wall temperature region less than 30°C or the high steam mass concentration presuming the oxygen combustion, the total heat transfer was higher than that predicted by the simple analogy correlation.

The thermal hydraulic behavior was experimentally studied in a heat exchanger for the latent heat recovery from a flue gas generated with the combustion of oxygen and A-oil. The steam mass concentration of the flue gas was approximately 25% which value was higher than that of an air-combustion flue gas. The parametric study varying the flue gas and feed water flow rate was conducted. Based on the previous basic studies, a prediction method for the heat exchanger was proposed[5]. In the prediction, the flue gas was treated as a mixture of CO_2, CO, O_2, SO_2 and H_2O, and the one-dimensional heat and mass balance calculation along the flow direction of flue gas was conducted. The heat and mass transfer on tubes was evaluated with a modified analogy correlation proposed in the previous basic study[4]. The modification was proposed to take account of the mass absorption effect at wall in the high steam mass concentration.

The following points are the difficulty associated with the calculation method and considered to be important in the verification comparing with the present experimental result.

1. Availability of the proposed analogy correlation between heat and mass transfer.
2. Proper estimation for physical properties and diffusivity of actual flue gas.
3. Precise calculation for the white fuming when the gas temperature merges with the saturation temperature.
4. Effect of condensate on heat transfer and pressure loss.
5. Stage by stage calculation method instead of conventional method using a logarithmic difference.

Experimental Apparatus and Method

Shown in Fig.2 is a schematic of experimental apparatus. The heat exchanger consisted of 2 staggered banks of 13 rows and 36 stages of spirally finned tubes as shown in Fig.3. The outer and inner diameters of the base tube installed with the fins are 20.2 and 25.4mm, respectively. The thickness and length of the plate fin are 1 and 8mm, respectively. To avoid the degradation of fin efficiency at the condensing region, the fin height was kept as small as possible. The flue gas from an oxygen combustion boiler is led to the upper plenum and flows downward in the first heat exchanger and upward in the second one. The flue gas was released to atmosphere from the outlet plenum.

Shown in Fig.4 is the arrangement of heat transfer tubes. The heat exchanger consists of a staggered bank of 13 row tubes and 72 stages in total. The 13 tubes at each stage are connected with a header to maintain the same flow rate of feed water. The feed water is supplied at the downstream of gas flow and flows counter-currently to the upstream. The temperature distributions of water and flue gas in the heat exchanger were measured with sheathed thermocouples. The thermocouple signals were transferred to a personal computer with a GPIB line and analyzed. The measurement error of the temperature in this study was within ±0.1 K. The pressure loss and the total amount of condensate generated in the heat exchanger were also measured.

The parametric study varying the flue gas flow rate, feed water temperature and flow rate was conducted. The major test conditions are shown in Table.1. The oxygen supplied to the boiler was produced wit PSA (pressure swing adsorption) method and the purity was approximately 97 % due to the inclusion of Argon gas. The oxygen ratio was maintained at approximately 1.05 and the flue gas flow rate was varied with changing the fuel flow rate in the boiler.

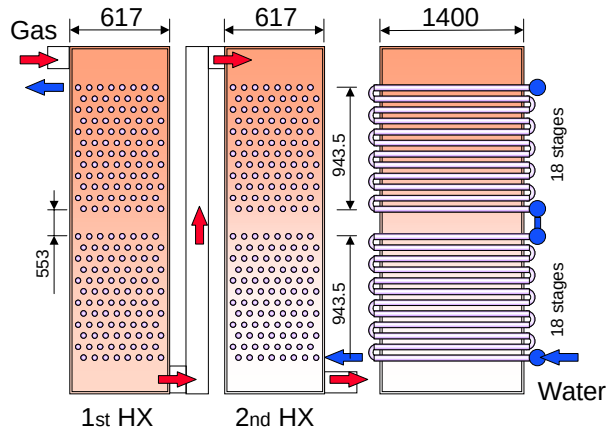

Fig. 2 Schematic of experimental apparatus

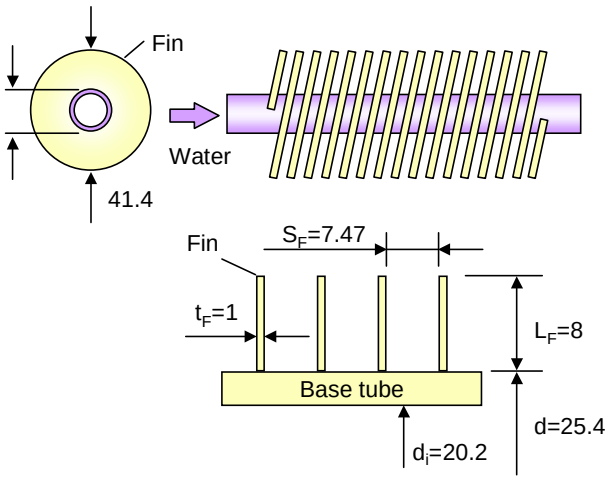

Fig. 3 Schematic of finned tubes

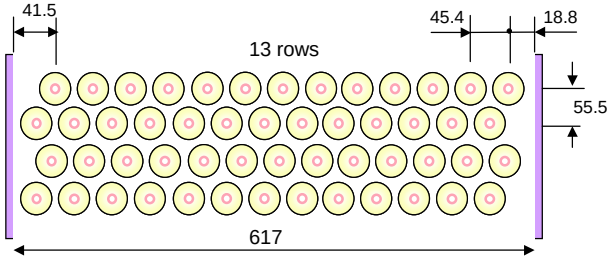

Fig. 4 Arrangement of heat transfer tubes

Table1 Major test conditions

Test no.	1	2	3	4
Load (%)	100	80	50	30
Oxygen ratio μ	1.05	1.05	1.05	1.05
Oxygen purity (%)	97.3	97.3	97.7	97.3
Fuel flow rate (kg/h)	1019	821	504	309
Gas inlet temp. (℃)	121.9	110.8	94.4	90.2
Feed water (kg/h)	11980	9480	6010	3590
Water inlet temp. (℃)	12.3	15.3	10.5	19.8

Table2 Properties of A-heavy oil fuel

	Fraction(kg/kg)
Carbon	F_C=0.861
Hydrogen	F_H=0.131
Sulfur	F_S=0.0063

Constitutive Equations for Prediction

Fuel combustion

The properties of A-heavy oil fuel used in the test boiler are shown in Table.2. Volumetric concentrations of CO_2, SO_2, O_2 and CO in the dry gas were measured by a gas analyzer. By using the mass flow rate of the fuel V_F, the volumetric flow rate of the carbon dioxide and monoxide, V_{COX} , is

$$V_{COX} = V_F \cdot \frac{F_C}{F_H} \cdot 22.4 \tag{1}$$

The volumetric flow rate of dry gas V_d is,

$$V_d = \frac{V_{COX}}{CO_2 + CO} \tag{2}$$

The molar fraction of the hydrogen corresponding to CO_X of 1 mol can be calculated as,

$$CHR = 12\frac{F_H}{F_C} \qquad \text{mol}$$

By using the measured concentration of CO_2, SO_2, O_2 and CO, the air ratio μ is calculated as

$$\mu = 1 + \frac{O_2 - 0.5CO}{(1 + CHR/4)(CO_2 + CO) + SO_2} \tag{3}$$

The volumetric fraction of H_2O in the flue gas can be estimated as

$$H_2O = \frac{(CO_2 + CO)\cdot CHR/2}{1 + (CO_2 + CO)\cdot CHR/2} \tag{4}$$

The volumetric flow rate of wet gas, V_{wt}, is

$$V_{wt} = \frac{V_d}{1 - H_2O} \tag{5}$$

When the flue gas temperature is T_f°C, the steam mass concentration C_f per unit volume of flue gas is,

$$C_f = \frac{H_2O \cdot 18}{22.4} \cdot \frac{273.15}{273.15 + T_f} \tag{6}$$

The steam mass concentration W_f per unit mass of flue gas is

$$w_f = \frac{H_2O \cdot 18}{H_2O \cdot 18 + (1 - H_2O)(CO_2 \cdot 44 + CO \cdot 28 + SO_2 \cdot 64 + O_2 \cdot 32)} \tag{7}$$

Heat and mass transfer in gas side

The total heat flux q_T consists of the convection heat flux q_V and the condensation heat flux q_C as

$$q_T = (q_V + q_C)(A_B + A_F\eta) \tag{8}$$

where η is the fin efficiency. The convection heat flux is expressed as

$$q_V = h_V(T_f - T_w) \tag{9}$$

The condensation heat flux q_C can be expressed as,

$$q_C = h_C L_W (C_f - C_w) \tag{10}$$

where C_w is the mass concentration of saturated steam at the wall temperature T_w of base tube.

The following empirical correlation[6] is available in the range of $2\times10^3 < Re_f \leqq 5\times10^5$.

$$Nu_f = j\,Re_f\,Pr_f^{0.33} \tag{11}$$

where
$$j = C_1C_3C_5\left(\frac{d + L_F}{d}\right)^{0.5} \tag{12}$$

$$C_1 = 0.25\,Re_f^{-0.35} \tag{13}$$

$$C_3 = 0.35 + 0.65e^{-0.25L_F/S_F} \tag{14}$$

$$C_5 = 0.7 \tag{15}$$

The fin efficiency can be calculated by,

$$\eta = Y_F\left[0.45\ln\left(\frac{d + L_F}{d}\right)(Y_F - 1) + 1\right] \tag{16}$$

where
$$Y_F = X_F(0.7 + 0.3X_F) \tag{17}$$

$$X_F = \frac{\tanh(mb)}{mb} \tag{18}$$

$$m = \left[\frac{2h}{\lambda_F t_F}\right]^{0.5} \tag{19}$$

$$b = L_F + t_F/2 \tag{20}$$

The fin efficiency strongly depends on the heat transfer coefficient, h, in Eq.(19). These correlations were obtained from the single-phase experiment where the heat flux is a simple multiple of the constant heat transfer coefficient and the temperature difference between wall and fluid. Although the condensation heat flux can not be expressed with the above simple relation, it is considered that the Eq.(19) with the larger heat transfer coefficient taking account of the condensation heat transfer would give an approximation. As a first attempt, the following equivalent heat transfer coefficient in the condensation region was used.

$$h = h_V + \beta \frac{h_C L_W (C_f - C_W)}{T_f - T_W} \quad (21)$$

where β=1 in the present calculation.

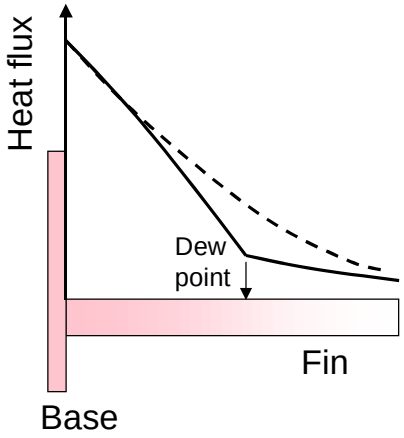

Fig. 5 Approximation of heat flux distribution

Shown in Fig.5 is a schematic image of heat flux distribution on a fin. The solid line depicts the heat flux distribution when the condensation takes place at the lower part of fin. As the dew point locates at the middle of fin, the heat flux sharply increases toward the base of fin from the dew point. The dash line is the calculated result with the equivalent heat transfer coefficient of Eq.(21). The heat flux at the fin base is the same as the actual heat flux shown by solid line and the heat flux gradually decreases toward the fin tip without the effect of dew point. Generally the fin efficiency evaluated with Eq.(21) yields slightly the higher value than the actual one due to the higher heat transfer coefficient including the condensation effect even in the dry region. However, at the white fuming condition when the saturation temperature merges with the gas temperature, the dew point never locate on the fin and the error due to the use of Eq.(21) becomes smaller.

For the condensation of steam on heat transfer tubes, the modified Sherwood number taking account of the mass absorption effect on the wall was proposed[4].

$$Sh_f = \frac{1}{1-w_i}\left(\frac{1-w_i}{1-w_f}\right)^{0.33} jRe_f\, Sc_f^{0.33} \quad (22)$$

Flue gas was treated as a mixture of CO_2, SO_2, O_2, CO and H_2O and its property was estimated with special combinations of each gas property proposed by the previous studies[7]. For example, the heat conductivity and the viscosity were estimated with the methods by Lindsay&Bromley[8] and Wilke[9], respectively. It is considered that a strong correlation exists between the thermal and mass diffusivities. As a. first attempt, the mass diffusivity of steam in flue gas was estimated with the well-known mass diffusivity of steam in air as

$$D = D_{air}\left(\frac{\kappa}{\kappa_{air}}\right) \quad (23)$$

where κ and κ_{air} are the thermal diffusivities of flue gas and air, respectively. The diffusivity of steam in air can be expressed as[10],

$$D_{air} = 7.65\times10^{-5}\frac{(T+273.15)^{11/6}}{P} \quad (24)$$

The one-dimensional heat and mass balance calculation along the flow direction of flue gas was conducted. The steam mass concentration and the flue gas temperature at N+1th stage can be calculated from those at Nth stage as shown in Fig.6.

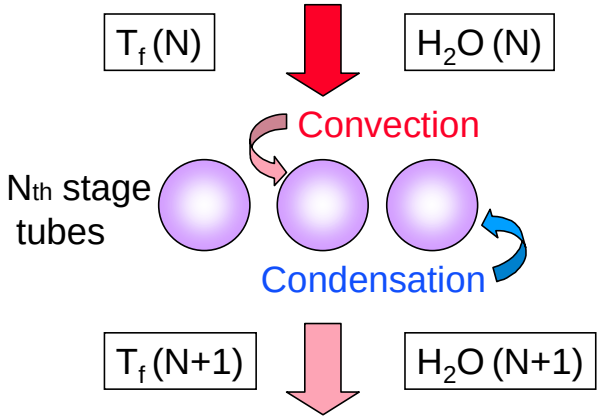

Fig. 6 One-dimensional calculation

The heat and mass balance equations are;

$$H_2O(N+1) = \frac{H_2O(N)\cdot V - \frac{q_C A_W}{L_W}\cdot\frac{22.4}{18}}{V - \frac{q_C A_W}{L_W}\cdot\frac{22.4}{18}} \quad (25)$$

$$T_f(N+1) = T_f(N) - \frac{q_V A_W}{C_{Pf}\rho_f (273.15+T_f)/273.15\cdot V} \quad (26)$$

where $A_w = A_B + A_F\eta$.

It is possible that the gas temperature merges with the dew point which is the saturation temperature corresponding to the partial pressure of steam in the flue gas. When the gas temperature decreases below the dew point, the condensation of steam in the flue gas takes place and the latent heat increases the gas temperature until the gas temperature coincides with the dew point. In this case, the energy balance gives the relation between the increase of the gas temperature, ΔT_f, and the decrease of steam concentration, ΔH_2O, as;

$$\Delta T_f = \frac{18}{22.4}\cdot\frac{L_W}{C_{Pf}\rho_f (273.15+T_f)/273.15}\cdot\Delta H_2O \quad (27)$$

Heat conduction in tube

The heat conductivity for the inconel or austenite stainless steel is given with the following approximate

correlation[11].

$$\lambda_t = 13.2 + 0.013T_t \quad \text{W/(m K)} \tag{28}$$

where T_t is the average temperature of tube as,

$$T_t = \frac{T_W + T_{Wi}}{2} \tag{29}$$

where T_w and T_{wi} are the outer and inner wall temperatures, respectively. The heat flux at the outer wall is,

$$q_W = \frac{2\lambda_t (T_W - T_{wi})}{d \ln(d/d_i)} \tag{30}$$

Heat transfer in water side

Heat transfer correlation by Dittus-Boelter taking account of the pipe inlet region is used. The coefficient by McAdams[12] is used for the modification.

$$Nu = 0.023\,Re^{0.8}\,Pr^{0.4}\left(1 + (\frac{d_i}{L})^{0.7}\right) \tag{31}$$

where L is the heating length of tube.

Pressure loss calculation

The pressure loss per a stage of tube is[13],

$$\Delta P = 2f\rho_f u^2 \tag{32}$$

where f is the friction factor. For the staggered bank of finned tube, the empirical correlation by ESCOA[6] is,

$$f = C_2 C_4 C_6 \left(\frac{d + L_F}{d}\right)^{0.5} \tag{33}$$

where $C_2 = 0.07 + 8\,Re_f^{-0.35}$ (34)

$$C_4 = 0.11\left[0.05\frac{S_1}{d}\right]^{-0.7(L_F/S_F)^{0.20}} \tag{35}$$

$$C_6 = 1.1 + \left[1.8 - 2.1e^{-0.15N_f^2}\right]e^{-2.0S_2/S_1} - \left[0.7 - 0.8e^{-0.15N_f^2}\right]e^{-0.6S_2/S_1} \tag{36}$$

Comparison of Experimental Result and Prediction

Temperature distribution

Shown in Fig.7 is the comparison of the experimental result and the prediction at 100% load. The solid lines are the temperatures of gas and water in the bank. The a-dot-dashed line and the two-dots-dashed line are the inner and outer wall temperature of base tubes, respectively. The dashed line is the saturation temperature (dew point) corresponding to the partial pressure of steam in the flue gas. As the outer wall temperature is smaller than the dew point, the condensation on the wall takes place throughout the heat exchanger. The dew point decreases with increasing stages as the steam concentration decreases. The key O and Δ are the measured temperatures of gas and water, respectively. The prediction for the water temperature agrees well with the experimental result. The prediction for the gas temperature is slightly higher than the experimental result in the second and fourth positions from the top. In these experiments of the high fuel flow rate, the entrained and dispersed condensate in the flue gas tends to wet the thermocouples among the tube bank. The wet thermocouples indicate the lower value than the actual gas temperature.

The average thickness of condensate was calculated with the method shown in APPENDIX. It was assumed that all the generated condensate flows on the tubes in the calculation. The maximum thickness was approximately 0.19mm. The existence of the film did not affect the calculated temperature profiles in the bank. The effect of condensate film on the tubes was considered to be negligibly small for the heat and mass transfer calculation.

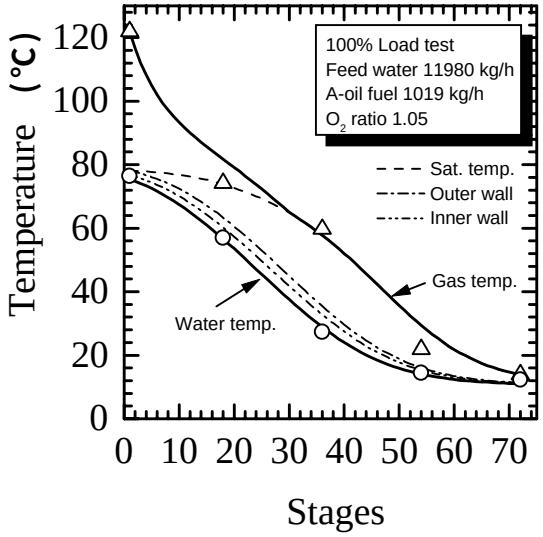

Fig. 7 Comparison of the experimental result and the prediction at 100% load

Shown in Figs.8 to 10 are comparisons of the experimental result and predictions when the fuel and feed water flow rate were reduced. When the flue gas flow rate and the amount of condensate are comparatively small, the effect of the wet thermocouple is considered to be negligible. The measured gas temperature agrees well with the prediction in the 50 and 30% load tests. This result also indicates the precise calculation for the white fuming condition when the saturation and gas temperature merge.

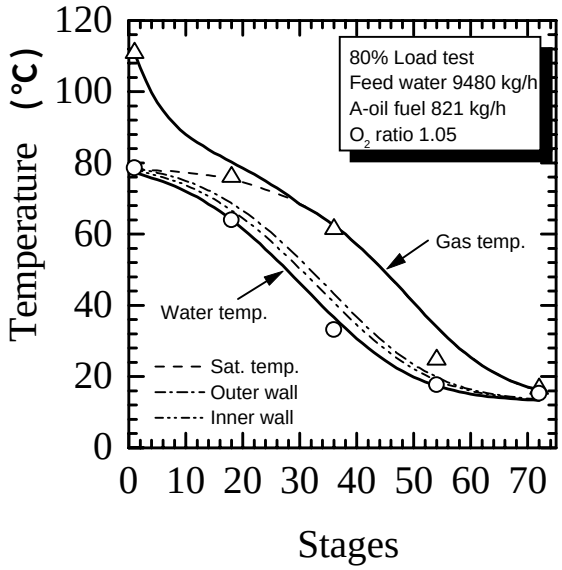

Fig. 8 Comparison of the experimental result and the prediction at 80% load

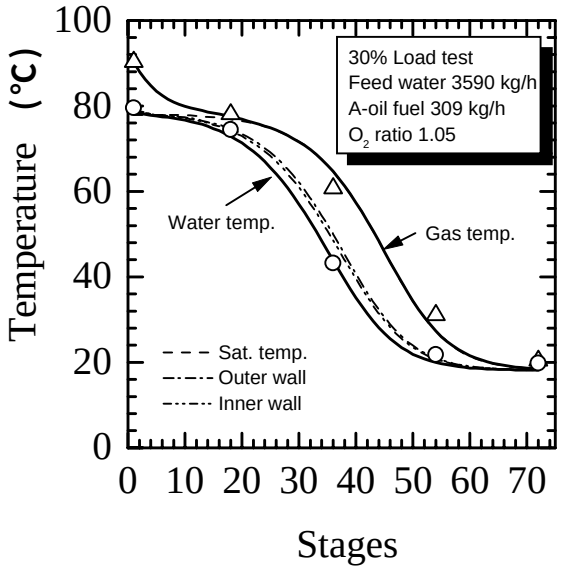

Fig. 10 Comparison of the experimental result and the prediction at 30% load

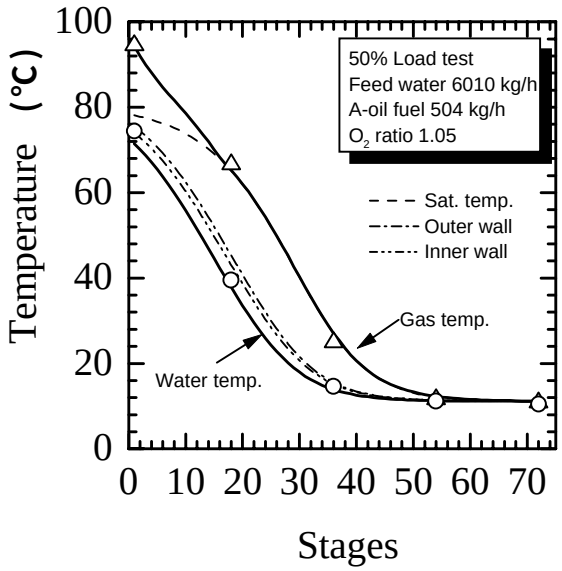

Fig. 9 Comparison of the experimental result and the prediction at 50% load

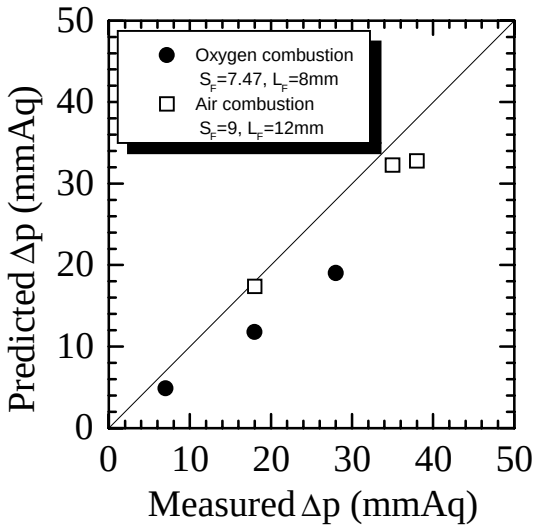

Fig. 11 Pressure difference between inlet and outlet of heat exchanger

Pressure loss and amount of condensate

Shown in Fig.11 is the comparison of experimental result and prediction for the pressure loss throughout the heat exchanger. The previous data[5] using air-combustion flue gas was also compared in the figure. The previous data was obtained in a bank of finned tubes where the fin space S_F was 9mm and the fin height L_F was 12 mm. As the empirical correlation obtained in the non-condensing region was used in the present one-dimensional calculation, the experimental results for the banks of finned tubes are slightly larger than the prediction. It is possible that the condensate between the fins increases the pressure loss in the bank. For the accurate prediction of pressure loss, the effect of condensate film on the tubes should be considered.

Shown in Fig.12 is the predicted and measured amount of condensate at each heat exchanger. The amount of condensate generated in the first heat exchanger was larger than that in the second one. The prediction slightly overestimates the generated amount at the second exchanger and agrees well with those at the first one.

Shown in Fig.13 is the comparison of experimental result and prediction for the amount of condensate throughout the heat exchanger. The total amount of

condensate generally agrees well with the one-dimensional mass and heat balance calculation proposed in the present study. The prediction indicates that the amount of condensate generated due to the white fuming was approximately 2% of the total.

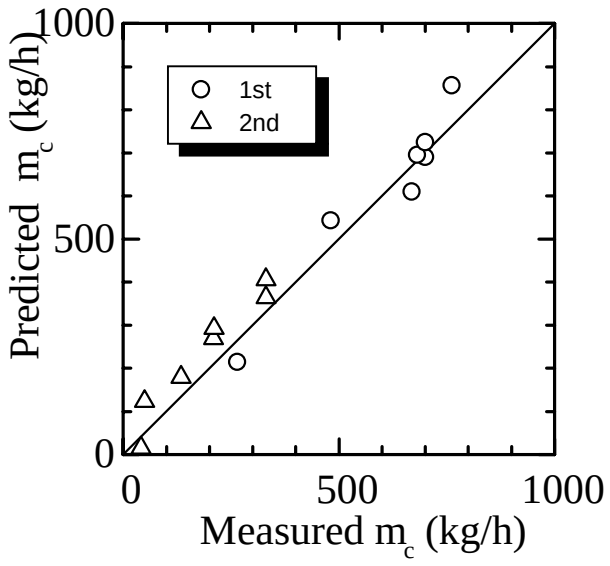

Fig. 12 Predicted and measured amount of condensate at each exchanger

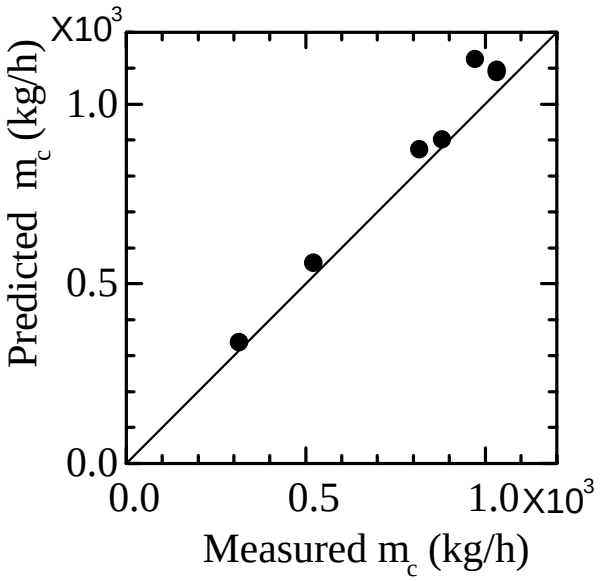

Fig. 13 Predicted and measured total amount of condensate

Conclusion

Thermal-hydraulic behavior of heat exchangers for the latent heat recovery was investigated experimentally by using an actual flue gas from an oxygen-combustion boiler. The parametric study varying the flue gas flow rate, feed water temperature and flow rate was conducted. Based on the previous basic studies, a prediction method for the heat exchanger was proposed. In the prediction, the flue gas was treated as a mixture of CO_2, CO, O_2, SO_2 and H_2O, and the one-dimensional heat and mass balance calculation along the flow direction of flue gas was conducted. The heat and mass transfer on tubes was evaluated with the modified analogy correlation. When the gas temperature decreased below the dew point, the condensation of steam in the flue gas took place and the released latent heat increased the gas temperature until the gas temperature coincided with the dew point. The effect of condensate film on the tubes was considered to be negligibly small for the heat transfer and pressure loss calculation. The experimental results for the temperature distributions of water and flue gas in the test heat exchangers with finned tubes agreed well with the prediction.

Acknowledgment

The authors appreciate the helpful supports by Kawasaki Thermal Engineering Co. Ltd., The Japan Society of Industrial Machinery Manufacturers and NEDO (New Energy and Industrial Technology Development Organization of Japan).

Nomenclature

A_B: heat transfer area of base tube [m^2]
A_F: heat transfer area of fin [m^2]
C: mass concentration per fluid of a unit volume [kg/m^3]
C_p: specific heat [J/kg]
d: outer diameter of base tube [m]
d_i: inner diameter of base tube [m]
D: mass diffusivity [m^2/s]
h_V: heat transfer coefficient [$W/(m^2K)$]
h_C: mass transfer coefficient [m/s]
L_F: fin height [m]
L_W: latent heat [J/kg]
Nu: Nusselt number [$= h_V d / \lambda$]
Nr: total number of stages
P: pressure [Pa]
q: heat flux [kW/m^2]
Pr: Prandtl number [$= \nu / \kappa$]
Re: Reynolds number [$= ud / \nu$]
S_1: spanwise pitch [m]
S_2: flow-directional pitch [m]
S_F: fin space [m]
Sh: Sherwood number [$= h_C d / D$]
Sc: Schmidt number [$= \nu / D$]
T: temperature [°C]
t: fin thickness [m]
u: velocity at minimum flow area [m/s]
V: volumetric flow rate [m_N^3/s]
w: steam mass concentration [kg/kg]
κ: thermal diffusivity [$= \lambda / (\rho C_P)$]
λ: heat conductivity [W/(mK)]
μ: oxygen ratio
ν: kinematic viscosity [m^2/s]
ρ: density [kg/m^3]

subscript
a: atmosphere
C: condensation
COX: carbon dioxide and monoxide,
d: dry gas
F: fuel or fin
f: flue gas
i: condensation surface
V: convection
W: outer wall of base tube
N: standard condition at 0°C and atmospheric pressure
sat: saturated condition of steam
sub: subcooling
wt: wet gas

References

1) Osakabe, M., Ishida, K., Yagi, K., Itoh, T. and Ohmasa, M., "Condensation heat transfer on tubes in actual flue gas (Experiment using flue gas at different air ratios)", (in Japanese), *Trans. of JSME* , 64-626, B, pp.3378-3383, 1998
2) Osakabe, M., Yagi, K., Itoh, T. and Ohmasa, M., "Condensation heat transfer on tubes in actual flue gas (Parametric study for condensation behavior)", (in Japanese), *Trans. of JSME* , 64-626, B, pp.3378-3383, 1999
3) Osakabe, M., Itoh, T. and Ohmasa, M., "Condensation heat transfer on spirally finned tubes in actual flue gas", (in Japanese), *J. of MESJ* , 35-4, pp.260-267, 2000
4) Osakabe, M., Itoh, T. and Yagi, K., "Condensation heat transfer of actual flue gas on horizontal tubes", *Proc. of 5th ASME/JSME Joint Thermal Eng. Conf., AJTE99-6397*, 1999
5) Osakabe, M., "Thermal-hydraulic behavior and prediction of heat exchanger for latent heat recovery of exhaust flue gas", *Proc. of ASME, HTD-Vol.364-2*, pp.43-50, 1999
6) ESCOA FINTUBE CORPORATION, SOLIDFIN HF. , 1979
7) JSME, Data Book: Heat Transfer 3rd Edition, (in Japanese) , 1983
8) Lindsay, A.L. and Bromley L.A., "Thermal conductivity of gas mixtures", *Indust. Engng. Chem*., 42, pp.1508-1510, 1950
9) Wilke, C.R., "A viscosity equation for gas mixture", *J. Chem. Phys*., 18, pp.517-519, 1950
10) Fujii, T., Kato, Y. and Mihara, K., "Expressions of transport and thermodynamic properties of air, steam and water", *Univ. Kyushu Research Institute of Industrial Science Rep.*66, pp.81-95, 1977
11) Osakabe, M., "Thermal-hydraulic study of integrated steam generator in PWR", *J. Nucl. Sci. & Technol.*, 26(2), 2 pp.86-294, 1989
12) McAdams, W.H., *Heat transmission*, McGRAW-HILL, 1954
13) Jakob, M., "Heat transfer and flow resistance in cross flow of gases over tube banks", *Trans. ASME*, 60, pp.381-392, 1938

Appendix

Though a part of condensate falls down between the tubes and on the duct wall, it is assumed that all the condensate generated at the upper stage flows on the tubes as a laminar film. The momentum balance dominated by viscous and gravity force gives the velocity distribution at θ° from the tube top:

$$u = \frac{(\rho_L - \rho_G) g \sin\theta}{\mu_L}\left(y\delta - \frac{y^2}{2}\right) \tag{37}$$

Integrating the above velocity profile and using the condensate mass flow rate per unit of tube length, m, yields

$$\delta = \left[\frac{1.5\mu_L m}{\rho_L(\rho_L - \rho_G) g \sin\theta}\right]^{1/3} \tag{38}$$

The heat conductivity of film is

$$K = \frac{\lambda_L}{\delta} = \left[\frac{{\lambda_L}^3 \rho_L(\rho_L - \rho_G) g \sin\theta}{1.5\mu_L m}\right]^{1/3} \tag{39}$$

The average conductivity from θ= 0° to θ=π is

$$\overline{K} = \frac{1}{\pi}\int_0^{\pi} K\, d\theta = 0.72\left[\frac{{\lambda_L}^3 \rho_L(\rho_L - \rho_G) g}{\mu_L m}\right]^{1/3} \tag{40}$$

The average heat resistance of film is defined as the inverse of the above average conductivity. The average film thickness is

$$\overline{\delta} = \frac{\lambda_L}{\overline{K}} \tag{41}$$

In the calculation, the mass flow rate, m, at a certain stage includes the condensate generated at the stage for the conservative estimation.

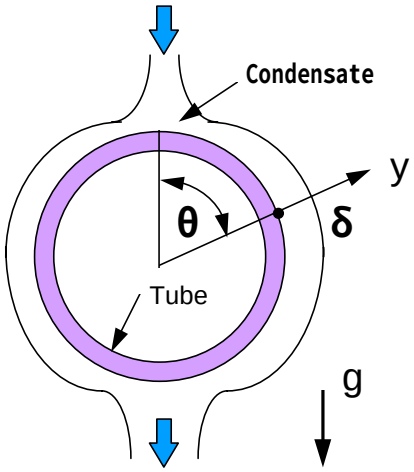

Fig. 14 Heat conductance of condensate film